35th Annual International Conference of the IEEE EMBS
Osaka, Japan, 3 - 7 July, 2013

Relation between Morphology of Sebaceous Glands inside Human Skin and Viscoelastic Properties

Ryo Nagaoka, Kazuto Kobayashi, and Yoshifumi Saijo, *Member, IEEE*

***Abstract*—Three-dimensional ultrasound microscopy with the central frequency of 120 MHz made it possible to observe *in vivo* sebaceous glands at the deep part of the dermis at microscopic level. The deformation displacements were measured by an established testing device, and the viscoelasticity was estimated from the measured displacements and Voigt model. The occupancy, density or average size of sebaceous glands was compared with the viscoleasticity. There were three major findings in the comparisons. First, the occupancy of sebaceous gland showed negative correlation with the elasticity. Second, the density of sebaceous glands showed positive correlation with the viscosity. Third, the average size of sebaceous glands showed negative correlation with the viscosity. In conclusion, viscoelastic property of human skin is strongly influenced by the morphology of the sebaceous glands.**

I. Introduction

The 3D ultrasound microscope enables to observe micro-structures of human skin such as sebaceous glands, hair follicles and capillary blood vessels with the high ultrasonic frequency of around 100 MHz [1-7]. Because the resolution is inversely proportional to the ultrasound frequency, 15 micron resolution is acquired by 100 MHz. In our previous paper [8,9], *in vivo* human skin morphology was evaluated by 3D ultrasound microscopy with the ultrasonic frequency of 120 MHz and its morphology was compared to the biomechanical properties measured by a biomechanical method [10, 11].

Viscoelastic properties of human skin are closely related to density, distribution, size and shape of sebaceous glands inside the dermis. However, there are few reports on relationship between the viscoelasticity and the morphology of sebaceous glands. The viscoelasticity of human skin can be measured by an established biomechanical testing method [11].

The objectives of the present study are to evaluate *in vivo* sebaceous glands morphology inside human skin by 3D ultrasound microscopy with the ultrasonic frequency of 120 MHz and to compare measured viscoelasticity and occupancy, density or average size of sebaceous glands inside human skin.

This project was supported in part by Grants-in-Aid for Scientific Research (Scientific Research (B) 22300175) from the Japan Society for the Promotion.

Ryo Nagaoka (Corresponding author, phone: +21-22-795-5882; fax: +81-22-795-7149; e-mail: ryo@ecei.tohoku.ac.jp) and Yoshifumi Saijo (e-mail: saijo@idac.tohoku.ac.jp) are with the Graduate School of Biomedical Engineering, Tohoku University, Sendai 980-8579 Japan.

Kazuto Kobayashi is with the Honda Electronics Co. Ltd., Toyohashi 441-3139 Japan (e-mail: kazuto@honda-el.co.jp).

II. Methods

A. Data Acquisition Setup

Table. 1 shows parameters for data acquisition. An electric impulse of pulser generated by a high speed switching semiconductor was used to excite P (VDF-TrFE) transducer for imaging. The reflection RF signals received by the transducer were introduced into the PC with A/D converter. Eight pulse echo sequences with 2000 sampling points were averaged for each scan line in order to increase the S/N ratio. The transducer was mounted on the X-Y scanner with two linear servo motors that were controlled by XY-scan controller connected to the serial port of the PC.

Table. 1 Parameters for data acquisition

Pulser	Rise time < 400 ps, width: 2 ns, voltage: 40 V, repetition rate: 10 kHz
Transducer	P(VDF-TrFE), aperture diameter: 2.4 mm, focal length: 3.2 mm, central frequency: 120 MHz, bandwidth (-6dB): 70-170 MHz
PC	Pentium D, 3.0 GHz, 2 GB RAM, 250 GB HDD
A/D	Acqiris DP210 (Geneva, Switzerland), frequency range: 500 MHz, smapling rate: 1GHz

Fig. 1 shows a block diagram of the 3D ultrasound microscope system.

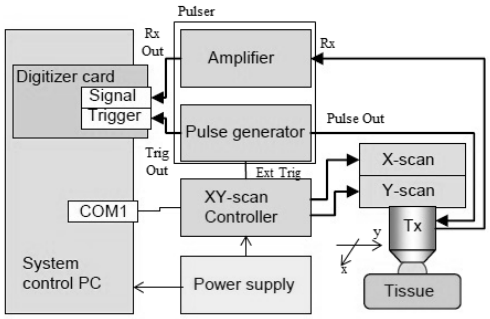

Fig. 1 Block diagram of 3D ultrasound microscope system

B. Image Processing

Obtained RF signals of each scanning line were converted to B-mode image by a conventional image processing algorithm of echography. A seal with quadrilateral hole at the center was pasted on the ROI of the skin. The scan area was 4.8 mm wide (X-axis) and 1.5 mm deep (Z-axis) with 300 x 300 pixels. Consecutive 150 B-mode images were reconstructed to volume data. It took a second to observe one B-mode image of the skin in the ROI, and 2 minutes to achieve full volume datum. The 3D ultrasound microscope system was

almost for real-time. Multi-planar reconstructed (MPR) images parallel to the skin surface were processed. The MPR images at 800-µm and 900-µm beneath the skin surface were observed because sebaceous glands mostly distributed in this layer. As the ex-vivo pilot study showed that the low intensity area corresponded to sebaceous gland, the sebaceous glands shown as low intensity regions in the MPR images were marked manually. The area and the number were measured by using image analysis software (Image J, NIH).

C. Measurement of Sebaceous Glands Morphology

Three parameters were calculated from the measured area and the number of the sebaceous glands; the occupancy, density and average size of sebaceous glands. These were given by following equations (1)-(3).

$$\text{Occupancy} = {}^{\text{Area [mm}^2\text{]}}\!/_{\text{ROI [mm}^2\text{]}} \quad (1)$$

$$\text{Desity [mm}^{-2}\text{]} = {}^{\text{Number}}\!/_{\text{ROI [mm}^2\text{]}} \quad (2)$$

$$\text{Average Size [mm}^2\text{]} = {}^{\text{Area [mm}^2\text{]}}\!/_{\text{Number}} \quad (3)$$

D. Skin Viscoelasticity Measurement

Human skin is consisted of three layers; epidermis, dermis and subcutis. Cutometer® (MPA580, Courage and Khazaka, Köln, Germany) was equipped for evaluating the mechanical properties of whole layers of skin [11]. This instrument measures the displacement on human skin surface during 3-second aspiration utilizing an optical measuring unit with a precision of 0.01 mm. The pressure value of the aspiration was set up to 300 kPa. The skin was vacuumed into the circular aperture (φ = 2 mm) by negative pressure from inside the probe gently put on the surface of the ROI. The skin returned to normal after the negative pressure was released. Fig. 2 shows the principle of measurement system.

Fig. 2 Principle of measurement system

The measured displacement was shown in Fig. 3 and was similar to step response of Voigt model. The displacement included whole changes of the epidermis, dermis and subcutis, and was measured as the averaged displacement in the ROI. A period during 3-second aspiration was defined as aspiration time and a period after 3-second aspiration was defined as release period. Voigt model is known as a viscoelastic model of living tissue. Viscosity and elasticity were calculated by fitting the displacement to the model respectively in two periods such as aspiration period and release period.

Each step response is represented by

$$s(t) = \frac{F}{E_r}\{1 - \exp\left(-\frac{E_r}{\eta_r}t\right)\} \text{ (aspiration period)} \quad (4)$$

and

$$s(t) = \frac{F}{E_f}\exp\left(-\frac{E_f}{\eta_f}t\right) \text{ (release period)}, \quad (5)$$

where s(t) is displacements generated by the suction, E_r and η_r are respectively elasticity and viscosity in aspiration period, and E_f and η_f are respectively elasticity and viscosity in release period. E_r , η_r , E_f and η_f were estimated from the displacement and the model under assumption of linear relationship between force (or pressure) and displacement (strain).

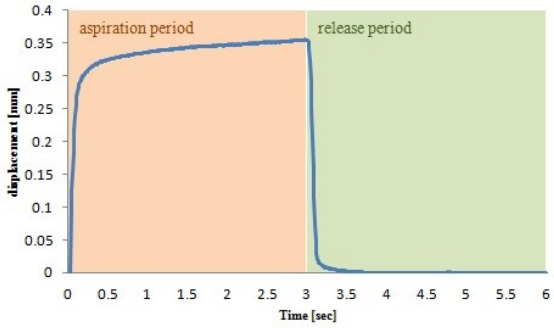

Fig. 3 Displacement measured by Cutometer®

D. Subjects

Twelve healthy male subjects with written informed consent (23.5 ± 0.6 year-olds) were evaluated by 3D ultrasound microscope. They didn't have significant skin diseases. The research was approved by an ethical committee of Tohoku University.

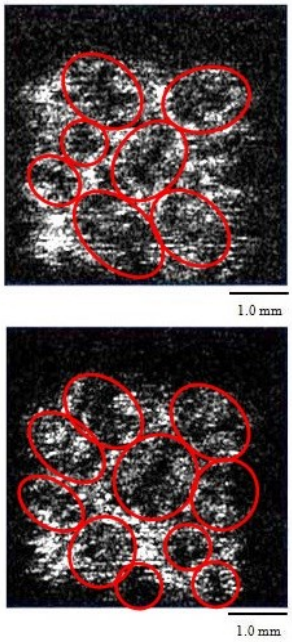

Fig. 4 MPR images of sebaceous glands inside normal skin of cheek (top) at 800-µm and (bottom) 900-µm beneath the surface

III. RESULTS

A. High Frequency Ultrasound Imaging

Fig. 4 shows the MPR images of 21-year old male's cheek at 800-μm and 900-μm beneath the skin surface. The imaged areas are 4.8 x 4.8 mm.

The *in vivo* sebaceous glands were able to be observed as low intensity regions in the MPR images, which were confirmed by past researches [3, 6, 8]. Each circle of the Fig. 4 corresponds to sebaceous glands of dermis.

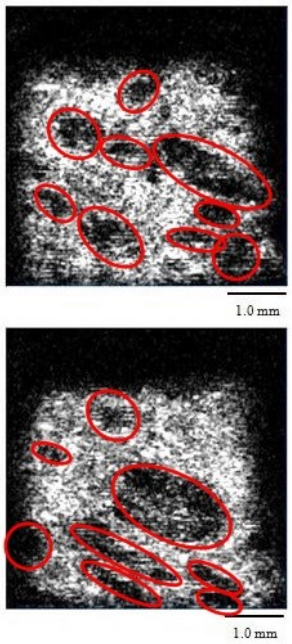

Fig. 5 MPR images of sebaceous glands inside normal skin of forearm at 800-μm (top) and 900-μm (bottom) beneath the surface

Fig. 5 shows the MPR images of 24-year old male's forearm at 800-μm and 900-μm beneath the skin surface. The imaged areas are 4.8 x 4.8 mm. Each circle of the Fig. 5 corresponds to sebaceous glands of dermis. The area of sebaceous glands of cheek is larger than that of forearm.

Fig. 6 is the graph showing occupancy and density of sebaceous glands in cheek and forearm at 800-μm beneath the skin surface.

Paired t-test was used to compare the measured values. The occupancy and density in cheek were significantly higher than those in forearm ($p < 0.01$). There was no significant difference in average size, which meant that the size was almost same both in cheek and forearm.

B. Skin Viscoelasticity

Fig. 7 shows the viscoelasticity of cheek and forearm. There was no significant difference in elasticity. The viscosity in release period was significantly higher than that in aspiration period at cheek ($p < 0.01$). Fig. 7 (bottom) showed significant differences in the value at forearm, and in that in release period ($p < 0.05$).

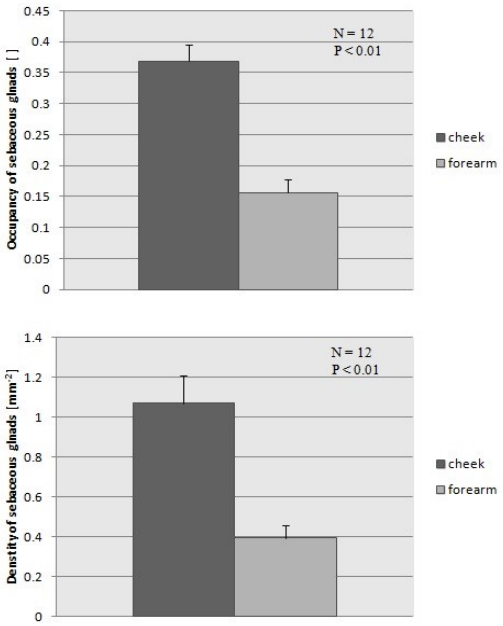

Fig. 6 Occupancy (top) and density (bottom) of sebaceous glands in cheek and forearm at 800-μm

C. Relation between the morphology and the Viscoelasticity

The relation in aspiration period was not shown. There were three major findings in consequence of comparisons between the sebaceous glands morphology and the viscoelastictiy. Fig. 8, 9 and 10 show the comparison results.

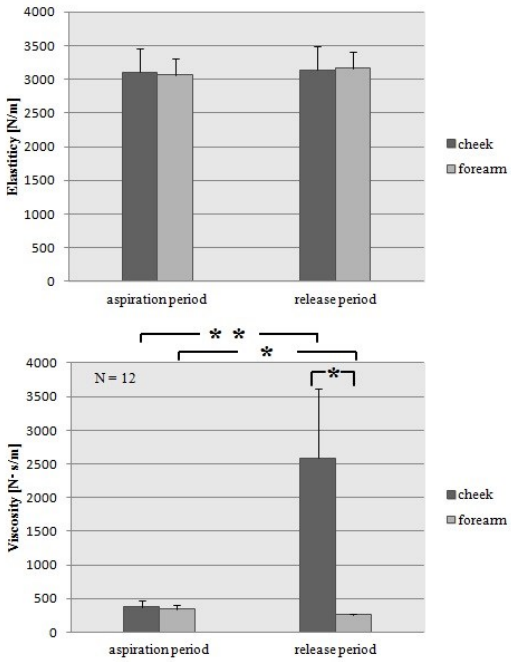

Fig. 7 Elasticity (top) and viscosity (bottom) of cheek and forearm

IV. DISCUSSION

The morphology of the sebaceous glands, occupancy, density and average size, can be observed by 3D ultrasound microscope. It's exactly adequate to measure skin

microstructures such hair follicles, sebaceous glands and capillary blood vessels.

The viscosity in release period was much higher than that in aspiration period at cheek. This leads to a view that the deformation in release period behaves like more similar properties of human skin to that in aspiration period. This reason is considered that the deformation is caused by forcible suction of Cutometer®.

Three major relationships were revealed by the comparisons. In forearm, the occupancy of sebaceous glands showed negative correlation with the elasticity (Fig. 8) and the density of sebaceous glands did positive correlation with viscosity (Fig. 9). The more the occupancy increases, the less the elasticity decreases, and the more the density increases, the more the viscosity decreases. Also in cheek, the average size of sebaceous glands showed negative correlation with the viscosity (Fig. 10), which meant that the more average size increases, the more the viscosity increase. The sebaceous glands play important roles on viscoelastic properties of human skin.

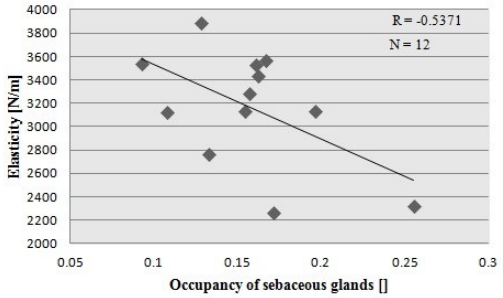

Fig. 8 Elasticity vs Occupancy of sebaceous glands in forearm at 800-µm

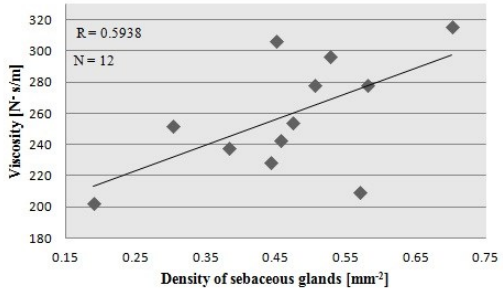

Fig. 9 Viscosity vs Density of sebaceous glands in forearm at 900-µm

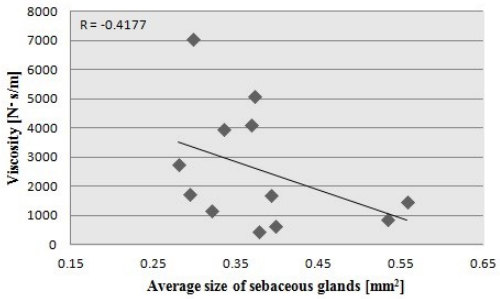

Fig. 10 Viscosity vs Average size of sebaceous glands in cheek at 900-µm

V. Conclusion

Sebaceous glands at deep part of the dermis in human skin were observed by three-dimensional ultrasound microscopy with the central frequency of 120 MHz. Viscoelasticity were estimated by fitting deformational displacements by Cutometer® to Voigt model. In release period the viscosity of cheek was higher than that of forearm. Three major correlations were revealed by comparisons between the morphology and the viscoelastic properties of human skin. These results suggest that an important role of sebaceous glands. High frequency ultrasound imaging contributes to the observation of human skin morphology, and the device befits the evaluation of human skin viscoelasticity.

References

[1] Y. Saijo, M. Tanaka, H. Okawai, H. Sasaki, S. Nitta and F. Dunn, "Ultrasonic tissue characterization of infracted myocardium by scanning acoustic microscopy," *Ultrasound Med Biol* 23 (1997), pp. 77-85.

[2] Y. Saijo, H. Sasaki, H. Okawai, S. Nitta and M. Tanaka, "Acoustic properties of atherosclerosis of human aorta obtained with high-frequency ultrasound," *Ultrasound Med Biol* 24 (1998), pp. 1061-1064.

[3] S. El Gammal, C. El Gammal, K. Kasper, C. Pieck, P. Altmeyer, M. Vogt and H. Ermert, "Sonography of the skin at 100 MHz enables *in vivo* visualization of stratum corneum and viable epidermis in palmar skin and psoriatic plaques," *J Invest Dermatol* 113 (1999), pp. 821-9.

[4] Y. Saijo, H. Sasaki, M. Sato, S. Nitta and M. Tanaka, "Visualization of human umbilical vein endothelial cells by acoustic microscopy," *Ultrasonics* 38 (2000), pp. 396-399.

[5] Y. Saijo, T. Ohashi, H. Sasaki, M. Sato, C. S. Jorgensen and S. Nitta, "Application of scanning acoustic microscopy for assessing stress distribution in atherosclerotic plaque," *Ann Biomed Eng* 29 (2001), pp. 1048-53.

[6] M. Vogt and H. Ermert, "In vivo ultrasound biomicroscopy of skin: spectral system characteristics and inverse filtering optimization," *IEEE Trans Ultrason Ferroelectr Freq Control* 54 (2007), pp. 1551-9.

[7] Y. Saijo, N. Hozumi, K. Kobayashi, N. Okada, E. D. Santos Filho, H. Sasaki, T. Yambe and M. Tanaka, "Ultrasonic tissue characterization of atherosclerosis by a speed-of-sound microscanning system," *IEEE Trans Ultrason Ferroelectr Freq Control* 54 (2007), pp. 1571-1577.

[8] K. Kumagai, H. Koike, Y. Kubo, R. Nagaoka, K. Kubo, K. Kobayashi and Y. Saijo, "Imaging of sebaceous glands of human skin by three-dimensional ultrasound microscopy and its relation to elasticity," *Conf Proc 33rd IEEE EMBC* (2011), pp7199-7202.

[9] K. Kumagai, H. Koike, R. Nagaoka, S. Sakai, K. Kobayashi and Y. Saijo, "High-resolution ultrasound imaging of human skin *in vivo* by using three-dimensional ultrasound microscopy," *Ultrasound Med Biol* 38 (2012), pp. 1833-8.

[10] P. G. Sator, J. B. Schmidt and H. Hönigsmann, "Comparison of epidermal hydration and skin surface lipids in healthy individuals and in patients with atopic dermatitis, *J Am Dermatol* 22, (1990), pp. 314-7.

[11] P. Elsner, D. Wilhelm and H. I. Maibach, "Mechanical properties of human forearm and vulvar skin," Br J Dermatol 46 (2003), pp. 352-8.